FOREX Publication
Open Access | Rapid and quality publishing

International Journal of
Electrical and Electronics Research (IJEER)
Research Article | Volume 12, Issue 4 | Pages 1240-1250 | e-ISSN: 2347-470X

Minimization of Harmonic in Stator current for Grid Connected Five Phase Squirrel Cage Induction Generator with Predictive Torque Control Technique

Chekuri Murali[1*], Pothula Jagadeesh[2] and Chintapudi Chengaiah[3]

[1]*Assistant Professor, EEE Department, S.R.K.R. Engineering College, Bhimavaram, Andhra Pradesh, India; chmvsraju@gmail.com*
[2]*Assistant Professor, EEE Department, S.R.K.R. Engineering College, Bhimavaram, Andhra Pradesh, India; jagadeesh.pothula@gmail.com*
[3]*Professor, EEE Department, SVU College of Engineering, Tirupati, Andhra Pradesh, India; chinthapudisvu@gmail.com*

***Correspondence:** Chekuri Murali ; *chmvsraju@gmail.com*

ABSTRACT- Wind energy systems have become a highly practical kind of renewable energy, which requires the development of more advanced control mechanisms to enhance efficiency and dependability. Five-phase machines provide several advantages compared to standard three-phase systems in this particular situation. These advantages include reduced torque variation, improved ability to handle faults, and increased capacity to handle power. The Direct Torque Control technology has attracted considerable interest for controlling five-phase squirrel cage induction generators employed in wind energy conversion systems. The main goal of DTC is to achieve efficient energy extraction from the wind by regulating torque and flux without the need for complex transformations and decoupling mechanisms, as required in field-oriented control. DTC is known for its simplicity and fast response, enabling high dynamic performance. This work introduces the notion of predictive torque control as a sophisticated control method for five-phase asynchronous generators in wind energy systems. to attain accurate control of stator flux torque control in the generator, which directly affects the efficiency of power generation. It uses predictive modelling to forecast the future torque needs of the generator, allowing for proactive modifications of control parameters to meet the expected demands. It improves power generation efficiency by precisely forecasting torque changes, minimizing torque ripples, and optimizing the generator's reaction to varying wind conditions. It facilitates accurate and efficient torque management, resulting in enhanced overall system performance. In this paper implementing predictive torque control in five-phase asynchronous generators in wind energy systems provides substantial advantages in terms of maintaining stator flux at its rated value, precise torque control, dynamic responsiveness, and reduced harmonics in stator currents.

Keywords: Direct Field Oriented Control (DFOC), Indirect Field Oriented Control (IFOC), Direct Torque Control (DTC), Squirrel Cage Induction Generator (SCIG), Predictive Torque Control (PTC).

ARTICLE INFORMATION

Author(s): Chekuri Murali, Pothula Jagadeesh and Chintapudi Chengaiah;

Received: 18/09/2024; **Accepted**: 28/10/2024; **Published**: 30/11/2024;
e-ISSN: 2347-470X;
Paper Id: IJEER 1809-18;
Citation: 10.37391/ijeer.120415
Webpage-link:
https://ijeer.forexjournal.co.in/archive/volume-12/ijeer-120415.html

1. INTRODUCTION

Wind power has emerged as a rapidly expanding form of renewable energy on a worldwide scale, playing a substantial role in curbing greenhouse gas emissions and advancing sustainable development. Due to the growing recognition of environmental concerns and the depletion of traditional energy sources, wind energy is now acknowledged as a vital element of renewable energy systems. Wind energy offers numerous benefits, such as its plentiful availability, widespread distribution, and little ecological footprint, making it a crucial contributor to the shift towards a low-carbon economy.

The worldwide capacity for wind power has been consistently increasing due to breakthroughs in technology, favourable government regulations, and reduced costs of wind turbine components. As reported by [1], the worldwide wind power capacity exceeded 743 GW by the conclusion of 2020, and further expansion is anticipated. Wind power has proven its capacity to provide a significant proportion of the global electricity requirements. Indeed, wind power currently accounts for about 20% of the total electricity generated in certain places [2]. Wind energy systems are commonly categorized as either onshore or offshore wind farms. Onshore wind energy is a firmly established and extensively utilized form of energy due to its cost-effective installation and convenient accessibility for maintenance [3]. Nevertheless, the advancement of offshore wind energy has recently garnered attention due to the elevated and more reliable wind velocities seen over oceanic areas. Offshore wind farms are expected to have a crucial impact on fulfilling future energy needs, especially in coastal areas [4]. An essential factor in wind energy integration is the efficient

FOREX Publication
Open Access | Rapid and quality publishing
International Journal of Electrical and Electronics Research (IJEER)
Research Article | Volume 12, Issue 4 | Pages 1240-1250 | e-ISSN: 2347-470X

connection of large-scale wind farms to the power grid. With the growing integration of wind energy into the energy mix, grid operators have difficulties associated with the fluctuating and irregular nature of wind power. To tackle these problems, different control strategies and power electronics technologies have been created to guarantee the stability of the grid and the seamless integration of wind power into current systems [5].

Squirrel Cage Induction Generators (SCIGs) are crucial components in renewable energy systems, namely in wind energy conversion systems (WECS). Due to their sturdy design, affordability, simple upkeep, and exceptional dependability, they are the favoured option for renewable energy applications compared to other types of generators. SCIGs are renowned for their uncomplicated rotor design, comprising of conductive bars that are connected by end rings, and their ability to function without requiring a distinct DC excitation scheme [6]

Multiphase Squirrel Cage Induction Generators are becoming more popular in renewable energy systems because they offer distinct benefits in enhancing system dependability, efficiency, and fault tolerance. Multiphase generators, commonly equipped with five, six, or more phases, offer greater flexibility than conventional three-phase systems, resulting in improved performance in challenging settings such as wind and maritime energy systems. [6] An intrinsic advantage of multiphase machines is their built-in fault-tolerant capability. Reliability is a crucial aspect in renewable energy applications, given that these systems are frequently installed in remote areas with restricted maintenance accessibility. Machine Side Converters (MSC) and Induction Generators also play a role in mitigating torque ripple, a notable problem in conventional three-phase generators. The implementation of a multiphase design ensures a more uniform distribution of the load throughout the different phases, leading to a smoother application of torque and a decrease in mechanical strain on the system.

The capacity of multiphase induction generators to scale up makes them a highly promising alternative to meet the increasing need for renewable energy. Utilizing multiphase induction generators in renewable energy systems provides enhanced power quality and less harmonics. Power quality is a crucial aspect of renewable energy systems that are connected to the grid. Insufficient power quality can result in inefficiency and even harm to delicate grid infrastructure. Utilizing multiphase systems can decrease the total harmonic distortion (THD) in the output current, resulting in a more pristine and consistent power generation [7]. Ensuring excellent power quality is crucial in micro grid applications, since it is necessary for the stable functioning of connected loads and equipment. Multiphase Induction Generators provide mechanical durability because of their simplified rotor design, which closely resembles that of conventional three-phase squirrel cage induction generators, in addition to its electrical advantages. The generator's design, which lacks brushes and slide rings, along with the robust squirrel cage rotor, makes it highly durable and requires no maintenance. This makes it ideal for withstanding challenging working circumstances, such as those encountered in offshore wind farms and tidal energy systems [8].

Five-phase Induction Generators have attracted considerable interest in renewable energy systems because of its improved reliability, ability to tolerate faults, and greater control capabilities. Due to the growing need for sustainable energy, especially in wind and tidal energy conversion systems, the benefits of five-phase make them a very appealing choice. The five-phase structure provides more flexibility than standard three-phase systems, resulting in enhanced performance in applications that require stability, power quality, and operational reliability [9]. The five-phase technology enables the generator to maintain operation at a lower capacity in the case of a phase failure, guaranteeing uninterrupted energy production and minimizing the chances of expensive downtime [10]. Five-phase induction generators have the additional benefit of being able to decrease harmonic distortion in the output power. Optimal power quality is essential for grid-connected renewable energy systems, as subpar power quality can result in inefficiencies, inflict harm on grid infrastructure, and diminish the stability of the power network [11].

The control of squirrel Cage Induction Generator can be classified into scalar and vector control techniques. Scalar control consists of variable voltage and variable frequency (V/F) control does not fulfil the control of regulating electromagnetic torque during various step change in wind speeds. Field oriented control consists of Direct Field Oriented Control Technique (DFOC) to decouple the control of flux and electromagnetic torque and Indirect Field Oriented Control Technique (IFOC) decouples the control of rotor flux and electromagnetic torque during various wind speeds. Field Orientation Control Technique controls only rotor flux. It is tedious to calculate parameters of rotor using stator quantities. Hence Direct Torque management (DTC) is new method for highly efficient management method used in renewable energy systems, specifically in wind energy conversion applications, to effectively manage Squirrel Cage Induction Generators (SCIGs). Direct torque control (DTC) presents numerous benefits such as rapid torque response, decreased reliance on machine characteristics, and the elimination of current control loops. [12]. DTC offers a strong answer to these difficulties by directly managing the electromagnetic torque and stator flux linkage, allowing for accurate control of the generator's performance even when the input conditions are unstable [13]. The main premise of DTC is to directly regulate torque and stator flux by choosing the most suitable voltage vectors, without relying on complicated transformations or proportional-integral (PI) controllers. This leads to a rapid and responsive reaction, which is crucial for wind turbines and other renewable energy systems that need to quickly respond to changing environmental conditions [14]. The capacity of DTC to provide rapid torque and flux responses also aids in reducing problems like torque ripple and mechanical strains, hence enhancing the overall dependability and durability of the system [15]. Implementing Direct Torque Control (DTC) in Squirrel Cage Induction Generators (SCIGs) has been demonstrated to enhance the electrical characteristics of grid-connected renewable energy systems. DTC, or Direct Torque Control, reduces harmonic distortions in the output power by offering exact control over torque and flux DTC enables the usage of PI-

FOREX Publication
Open Access | Rapid and quality publishing
International Journal of Electrical and Electronics Research (IJEER)
Research Article | Volume 12, Issue 4 | Pages 1240-1250 | e-ISSN: 2347-470X

Controllers to regulate stator flux and electromagnetic torque. To eliminate the usage of PI- Controllers new control technique is proposed. *i.e.* Predictive Torque Control (PTC) technique.

Predictive Torque Control (PTC) has become a dominant control method for Squirrel Cage Induction Generators (SCIGs), especially in renewable energy systems such as wind and hydroelectric power. PTC is a control approach that uses models to forecast system behaviour in real-time [16].

Conventional control techniques, such as direct torque control (DTC) or vector control, encounter challenges in maintaining optimal performance in these circumstances. PTC, in contrast, enhances dynamic performance by utilizing model-based algorithms to accurately forecast and regulate the torque and flux of SCIGs [17]. This feature is crucial for guaranteeing effective energy acquisition and distribution in renewable energy systems that operate at different speeds [18]. During each control step, the system chooses the most efficient switching state of the inverter that minimizes a predetermined cost function. This cost function usually considers variables such as torque error, flux error, and switching losses. The utilization of PTC (Predictive Torque Control) yields precise regulation of torque and flux, ensuring superior performance with minimal fluctuations [19]. PTC's ability to swiftly adapt to changing operating conditions makes it highly effective in wind energy systems, which often experience frequent variations in wind speed [20]. Ensuring a reliable and efficient energy conversion process is of utmost importance in wind energy systems. PTC can dynamically adjust torque control in real-time, guaranteeing that the SCIG functions at its utmost efficiency across different wind speeds. [21]. PTC offers notable benefits due to its adaptability in addressing diverse control objectives, including loss minimization, torque ripple reduction, and seamless transitions during system disruptions. In addition, PTC obviates the necessity for modulation stages or proportional-integral (PI) controllers, which are commonly used in conventional control techniques. [22].

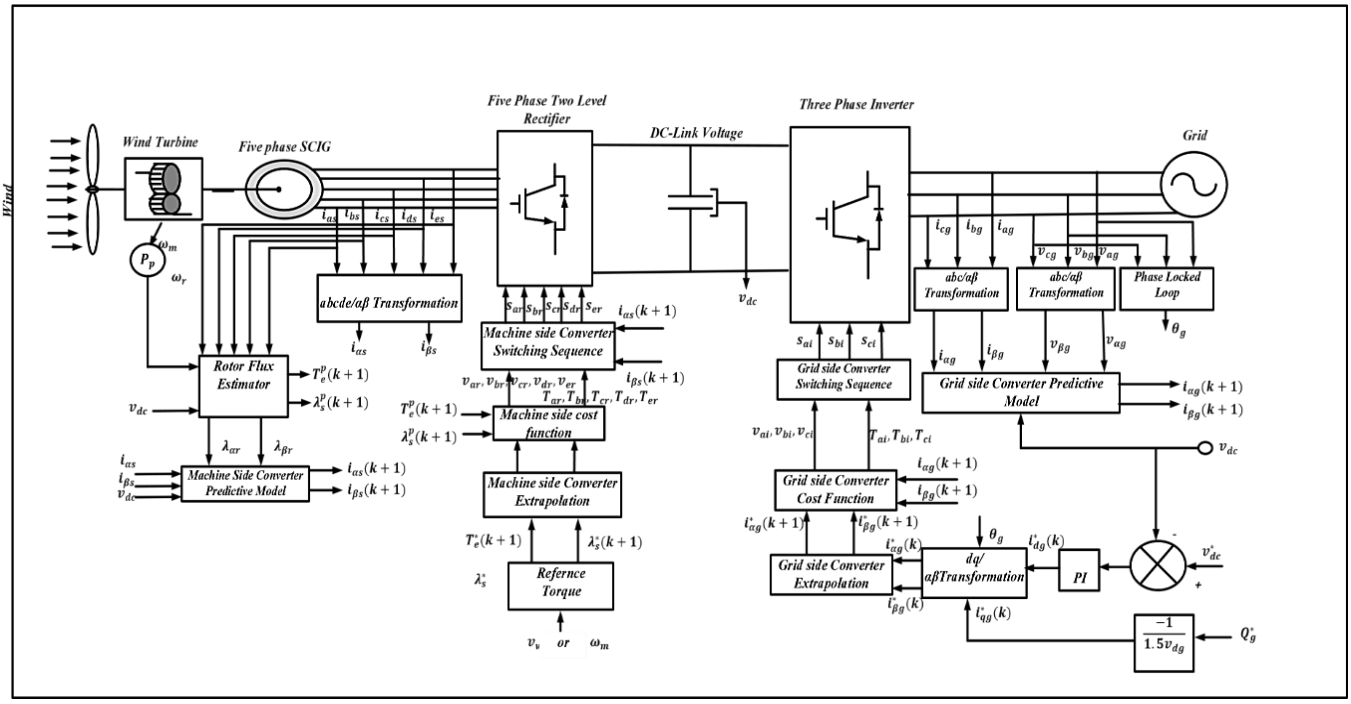

Figure 1. Schematic Block Diagram for Predictive Torque Control based Five Phase Asynchronous Generator

2. MATHEMATICAL MODEL OF WIND TURBINE

Incorporating the concept of *Cp* (Coefficient of Performance) enables the formulation of a precise mathematical model for the wind turbine. The potential energy of air moving through a wind turbine with a surface area of A and a speed of V m/sec can be expressed as

$$P_w = 0.5\rho AV^3 \quad (1)$$

Where,
P_w : wind power
A: area swept by blades
V: speed of the wind
ρ: air density - kg/m^3

The power coefficient of the turbine, denoted as *Cp* (λ, β), demonstrated by the pitch angle (β) & the tip-speed ratio (λ). The article describes the wind energy captured by the wind turbine.

$$\lambda = \frac{\omega_t R}{V} \quad (2)$$

ω_t the turbine speed is measured in radians/second.

FOREX Publication
Open Access | Rapid and quality publishing
International Journal of Electrical and Electronics Research (IJEER)
Research Article | Volume 12, Issue 4 | Pages 1240-1250 | e-ISSN: 2347-470X

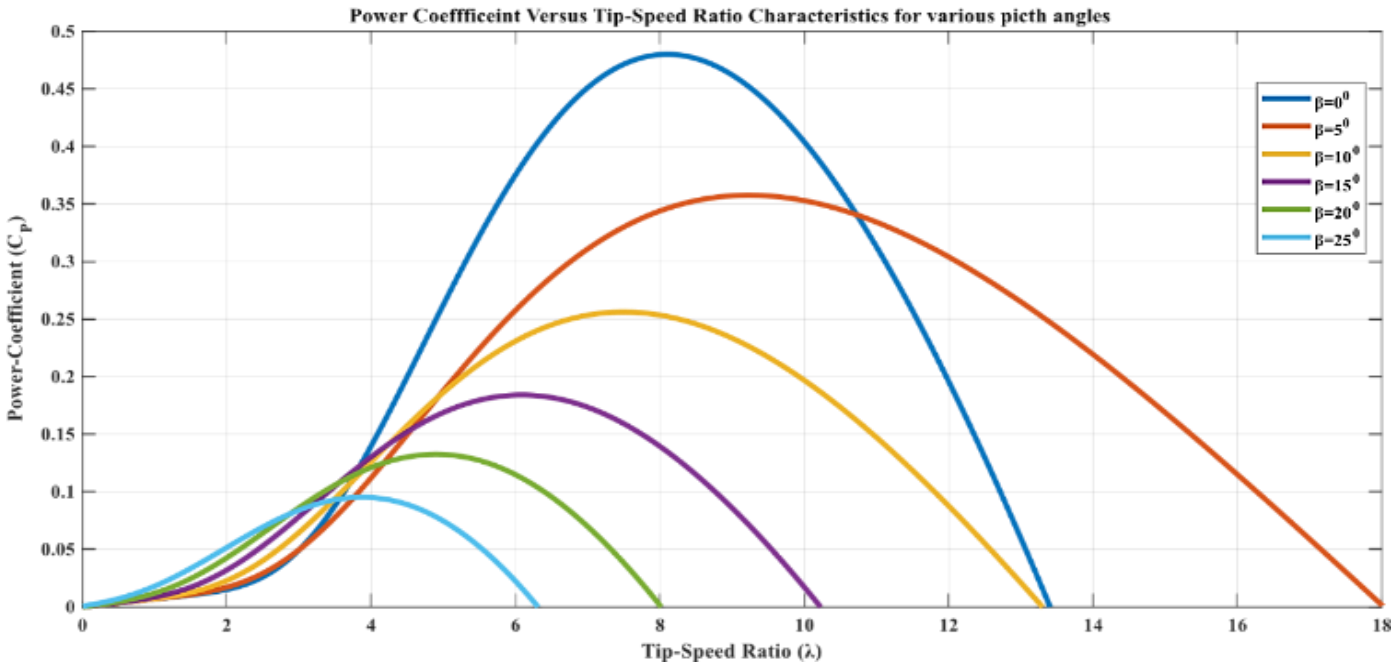

Figure 2. Power coefficient characteristic for different pitch angles

From *figure 2* it is noticed that the maximum power co-efficient of wind turbine is 0.49 at pitch angle $\beta = 0^0$. *Equation (1)* indicates that the mechanical power of the wind turbine is directly proportional to the cube of the wind velocity. During cut-in wind speed 6 m/sec to rated wind speed *i.e.* 13 m/sec the pitch angle is maintained at 0^0 to extract the maximum mechanical power from the wind. When wind speed increases beyond rated value i.e. 13 m/sec the mechanical power of the wind turbine is also increases as it is proportional to the cube of the wind velocity. To limit the mechanical power of the wind turbine the pitch angle β is increased step by step Wind-powered machinery is provided with mechanical power by

$$P_m = 0.5\rho A V^3 C_P(\lambda, \beta) \quad (3)$$

Where,

C_P : coefficient power

β : Pitch angle of blade

$$C_P = 0.517\left(\frac{116}{\lambda_i} - 0.4\beta - 5\right)e^{-\frac{21}{\lambda_i}} + 0.068\lambda$$

$$\frac{1}{\lambda_i} = \frac{1}{\lambda + 0.08\beta} - \frac{0.035}{\beta^3 + 1}$$

P_m : Mechanical power and

ω_t : Mechanical speed of turbine

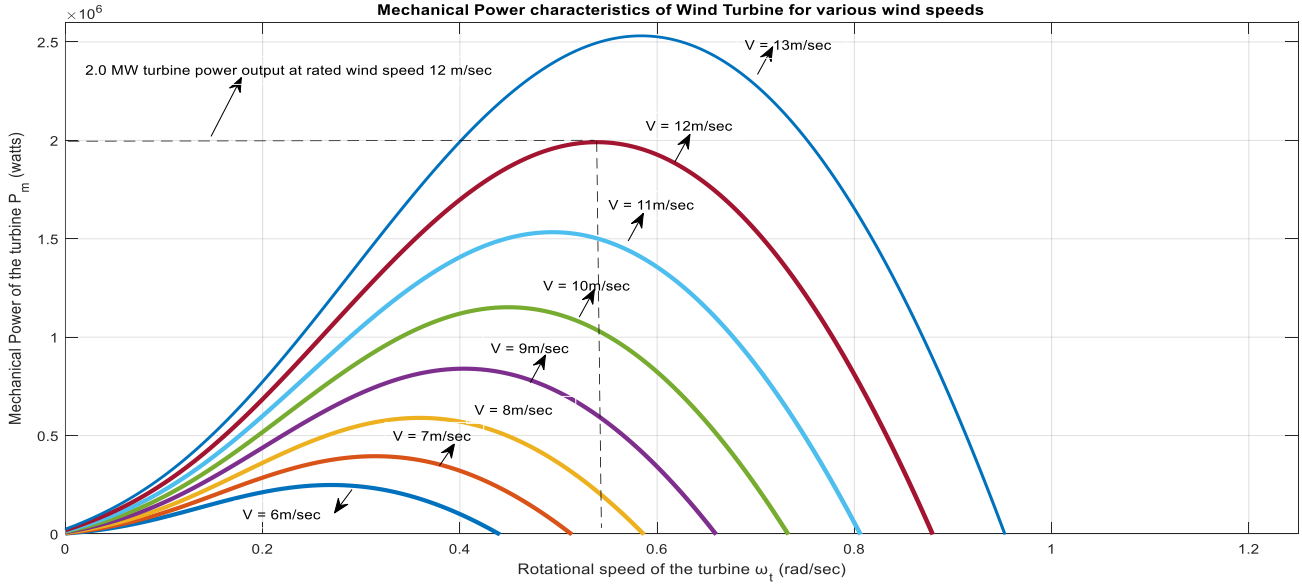

Figure 3. Mechanical Power Characteristics for different wind speeds

FOREX Publication
Open Access | Rapid and quality publishing
International Journal of Electrical and Electronics Research (IJEER)
Research Article | Volume 12, Issue 4 | Pages 1240-1250 | e-ISSN: 2347-470X

Figure 3 shows the mechanical power characteristics of wind turbine for wind speeds varies from 6 m/sec to 13 m/sec. The wind turbine produces the maximum mechanical power of 2.0 Mega Watts (MW) for wind speed 12 m/sec. If mechanical power of wind turbine exceeds rated mechanical power due to increase in wind speed it should be maintained at rated value by adjusting pitch angle β. The generated mechanical power of the wind turbine during various wind speeds shown in *figure 3*. is fed to the five-phase squirrel cage induction generator to generate the electrical power. The reference torque is generated from the mechanical power and is considered as negative value.

3. DISCRETE MATHEMATICAL MODELLING OF FPSG

The dynamic equations of an FPSG expressed [23] in terms of d-q model on stator and rotor side Stator side voltage equations are

$$v_{ds} = i_{ds}r_s + p\lambda_{ds} - \omega_s\lambda_{qs} \quad (4)$$

$$v_{qs} = i_{qs}r_s + p\lambda_{qs} + \omega_s\lambda_{ds} \quad (5)$$

Rotor side voltage equations are

$$v_{dr} = i_{dr}r_r + p\lambda_{dr} - (\omega_s - \omega_r)\lambda_{qr} \quad (6)$$

$$v_{qr} = i_{qr}r_r + p\lambda_{qr} + (\omega_s - \omega_r)\lambda_{dr} \quad (7)$$

$$\lambda_{ds} = (L_{ls} + L_m)i_{ds} + L_m i_{dr}$$

$$\lambda_{qs} = (L_{ls} + L_m)i_{qs} + L_m i_{qr}$$

$$\lambda_{dr} = (L_{lr} + L_m)i_{dr} + L_m i_{ds}$$

$$\lambda_{qr} = (L_{lr} + L_m)i_{qr} + L_m i_{qs}$$

Where

v_{ds} : d-axis of stator voltage

v_{qs} : q-axis of stator voltage

v_{dr} : d-axis of rotor voltage

v_{qr} : q-axis of rotor voltage

λ_{ds} : d-axis of stator flux linkage

λ_{qs} : q-axis of stator flux linkage

λ_{dr} : d-axis of rotor flux linkage

λ_{qr} : q-axis of rotor flux linkage

i_{ds} : d-axis of stator current

i_{qs} : q-axis of stator current

i_{dr} : d-axis of rotor current

i_{qr} : q-axis of rotor current

Transient conditions occur in FPSG due to sudden changes in wind speed or other disturbances. The *equation (4)* to *equation (7)* determines the transient conditions of five-phase squirrel cage induction generator (FPSG). To control the FPSG during transient change in wind speeds PI- controllers will be used. PI controllers may not perform optimally during transitory periods, and their sluggish response time may hinder their ability to promptly adapt to abrupt system changes.

In this research study, the aim is to address the elimination of PI-controllers in Wind Energy Conversion Systems (WECS) by implementation of Model Predictive Control (MPC). Model Predictive Control (MPC) dynamically adjusts control actions in response to real-time measurements, allowing the system to rapidly adapt to changing wind speed conditions.

To implement Model Predictive Control (MPC) for an FPSG the dynamical *equation (4)* to *equation (7)* should be discretized by sampling methods. It is not possible to discretize the dynamical *equation (4)* to *equation (7).* Hence the dynamic equations of the induction generator [23] can be expressed in terms of stator current and rotor flux as state variables shown in *equation (8)* need to be discretized using sampling methods. The state variables can be expressed in terms of the stator current and rotor flux as indicated by [24].

$$\begin{bmatrix} \dot{i}_{\alpha s}(t) \\ \dot{i}_{\beta s}(t) \\ \dot{\lambda}_{\alpha r}(t) \\ \dot{\lambda}_{\beta r}(t) \end{bmatrix} = \begin{bmatrix} -\frac{1}{\tau_\sigma} & 0 & \frac{K_r}{\sigma L_s \tau_r} & \frac{K_r \omega_r(t)}{\sigma L_s} \\ 0 & -\frac{1}{\tau_\sigma} & -\frac{K_r \omega_r(t)}{\sigma L_s} & \frac{K_r}{\sigma L_s \tau_r} \\ \frac{L_m}{\tau_r} & 0 & -\frac{1}{\tau_r} & -\omega_r(t) \\ 0 & \frac{L_m}{\tau_r} & \omega_r(t) & -\frac{1}{\tau_r} \end{bmatrix} \begin{bmatrix} i_{\alpha s}(t) \\ i_{\beta s}(t) \\ \lambda_{\alpha r}(t) \\ \lambda_{\beta r}(t) \end{bmatrix} + \begin{bmatrix} \frac{1}{\sigma L_s} & 0 \\ 0 & \frac{1}{\sigma L_s} \\ 0 & 0 \\ 0 & 0 \end{bmatrix} \begin{bmatrix} v_{\alpha s}(t) \\ v_{\beta s}(t) \end{bmatrix} \quad (8)$$

Where,

$i_{\alpha s}$, $i_{\beta s}$: stator currents of FPSG in stationary reference frame

$\lambda_{\alpha r}$, $\lambda_{\beta r}$: rotor flux linkages of FPSG in stationary reference frame

$v_{\alpha s}$, $v_{\beta s}$: stator voltages in α-β reference frame

ω_r: rotor speed

L_m: Mutual leakage inductance between stator and rotor

L_s: stator inductance

τ_σ: stator transient time constant = $\underline{\sigma L_s}$

$r_\sigma = R_s + k_r^2 R_r$

τ_r: rotor time constant $= \frac{L_r}{R_r}$

FOREX Publication
Open Access | Rapid and quality publishing
International Journal of Electrical and Electronics Research (IJEER)
Research Article | Volume 12, Issue 4 | Pages 1240-1250 | e-ISSN: 2347-470X

K_r: rotor coupling coefficient = $\frac{L_m}{L_r}$

σ: leakage factor = $1 - K_s K_r = 1 - \frac{L_m^2}{L_s L_r}$

The stator flux in stationary reference frame can be obtained using state variables of stator current and rotor flux as

$$\begin{bmatrix}\lambda_{\alpha s}(t)\\ \lambda_{\beta s}(t)\end{bmatrix} = \begin{bmatrix}\sigma L_s & 0 & K_r & 0\\ 0 & \sigma L_s & 0 & K_r\end{bmatrix}\begin{bmatrix}i_{\alpha s}(t)\\ i_{\beta s}(t)\\ \lambda_{\alpha r}(t)\\ \lambda_{\beta r}(t)\end{bmatrix} \quad (9)$$

Where

$\lambda_{\alpha s}$, $\lambda_{\beta s}$: stator flux linkages in stationary reference frame
L_s : stator leakage inductance using *equation (9)* the Electromagnetic Torque for FPSG in terms of rotor flux and stator current state variable can be expressed as

$$T_e = \frac{5}{2} P L_m \left(i_{\alpha s}\lambda_{\beta r} - i_{\beta s}\lambda_{\alpha r}\right) \quad (10)$$

$$T_e - T_L = J\frac{d\omega_m}{Pdt} \quad (11)$$

Where,

T_e: Electromagnetic torque
T_L: Load torque
J : Moment of Inertia

The FPSG sampled-data in discretization method with Forward Euler discretization is given by [24]

$$\begin{bmatrix}i_{\alpha s}^p(k+1)\\ i_{\beta s}^p(k+1)\\ \lambda_{\alpha r}^p(k+1)\\ \lambda_{\beta r}^p(k+1)\end{bmatrix} = \phi_s \begin{bmatrix}i_{\alpha s}^p(k)\\ i_{\beta s}^p(k)\\ \lambda_{\alpha r}^p(k)\\ \lambda_{\beta r}^p(k)\end{bmatrix} + \Gamma_s \begin{bmatrix}v_{\alpha s}^p(k)\\ v_{\beta s}^p(k)\end{bmatrix} \quad (12)$$

$$\phi_s = \begin{bmatrix}1-\frac{T_s}{\tau_\sigma} & 0 & \frac{K_r T_s}{\sigma L_s \tau_r} & \frac{K_r \omega_r T_s}{\sigma L_s}\\ 0 & 1-\frac{T_s}{\tau_\sigma} & -\frac{K_r \omega_r T_s}{\sigma L_s} & \frac{K_r T_s}{\sigma L_s \tau_r}\\ \frac{L_m T_s}{\tau_r} & 0 & 1-\frac{T_s}{\tau_r} & -\omega_r T_s\\ 0 & \frac{L_m T_s}{\tau_r} & \omega_r T_s & 1-\frac{T_s}{\tau_r}\end{bmatrix}$$

$$\Gamma_s = \begin{bmatrix}\frac{T_s}{\sigma L_s} & 0\\ 0 & \frac{T_s}{\sigma L_s}\\ 0 & 0\\ 0 & 0\end{bmatrix}$$

Where,

$i_{\alpha s}^p(k+1)$ and $i_{\beta s}^p(k+1)$:Predicted stator current using (k+1) sampling instant in stationary reference frame
$\lambda_{\alpha r}^p(k+1)$ and $\lambda_{\beta s}^p(k+1)$: Predicted rotor fluxes using (k+1) sampling instant in stationary reference frame
$v_{\alpha s}^p(k)$ and $v_{\beta s}^p(k)$ are predicted stationary reference frame stator voltages in discrete time
$i_{\alpha s}^p(k)$ and $i_{\beta s}^p(k)$: are predicted stationary reference frame stator currents in discrete time
$\lambda_{\alpha r}^p(k)$ and $\lambda_{\beta r}^p(k)$: are predicted stationary reference frame rotor fluxes in discrete time
T_s : discretized sample time

The stator flux in discrete time can be expressed as

$$\begin{bmatrix}\lambda_{\alpha s}(k)\\ \lambda_{\beta s}(k)\end{bmatrix} = \begin{bmatrix}\sigma L_s & 0 & K_r & 0\\ 0 & \sigma L_s & 0 & K_r\end{bmatrix}\begin{bmatrix}i_{\alpha s}(k)\\ i_{\beta s}(k)\\ \lambda_{\alpha r}(k)\\ \lambda_{\beta r}(k)\end{bmatrix} \quad (13)$$

Where, $\lambda_{\alpha s}(k)$ & $\lambda_{\beta s}(k)$: stationary reference frame stator flux in discrete time *equations (8)* to *equation (13)* gives the dynamical behavior of FPSG in discrete time domain to implement predictive torque control.

4. DISCRETE MATHEMATICAL MODELLING OF FIVE PHASE TWO LEVEL VOLTAGE SOURCE RECTIFIER

A five-phase two-level voltage source rectifier (VSR) is employed for the control of a full power synchronous generator (FPSG) employing model predictive control. A five-phase variable speed drive (VSR) consists of five separate and independent phase legs. Each leg is accountable for producing a voltage waveform for its corresponding phases.

In general, to operate three phase inverter using space vector PWM technique it requires $2^3 = 8$ switching states are used for producing PWM signal. Similarly, for Five-Phase rectifier it requires $2^5 = 32$ switching states are used for producing PWM signals in five phase supply and corresponding switching states are shown in *figure 4*. In the model predictive control of a FPSG, the switching states consists of five phase space vector PWM consists of inner decagon, middle decagon, and outer decagon [25]. The switching states of inner decagon consists of small vectors which are lower in magnitude. The switching states of middle decagon consists of medium voltage vectors. The switching states are in inner and middle decagon are not sufficient to generated the required voltages in magnitude for FPSG in transient wind speed conditions. Inner decagon and Middle decagon switching state vectors generate less voltage than outer polygons. Hence inner decagon and middle decagon switching state vectors are not used to generate required output voltages for the rectifier. Switching states are located at outer decagon around the 360^0 with the phase displacement of 36^0 are shown in *figure 4* [25]. The resultant vectors of switching states

FOREX Publication
Open Access | Rapid and quality publishing
International Journal of Electrical and Electronics Research (IJEER)
Research Article | Volume 12, Issue 4 | Pages 1240-1250 | e-ISSN: 2347-470X

around the outer decagon are $\frac{4}{5}v_{dc}\exp 0^0$, $\frac{4}{5}v_{dc}\exp 36^0$, $\frac{4}{5}v_{dc}\exp 72^0$, $\frac{4}{5}v_{dc}\exp 108^0$ etc around 360^0 corresponding to space vector diagram shown in *figure 4* and are tabulated in *table 1*. These switching states are located around the outer decagon are applied for five phase rectifiers to generate necessary PWM signals in order to inject five phase voltages to FPSG.

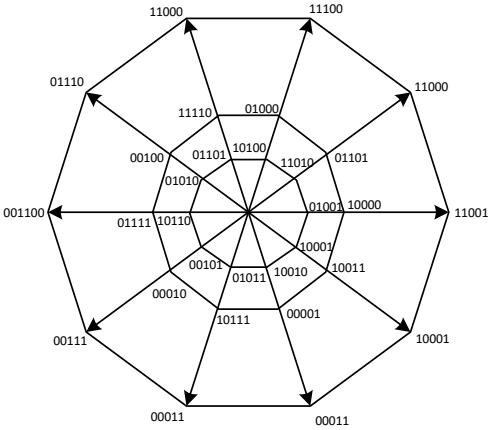

Figure 4. Space Vector Diagram for Five phase Voltage Source Rectifier

Table 1. Vector Locations of Five Phase Voltage Source Rectifier

Switching state						
S.No	S_a	S_b	S_c	S_d	S_e	**Resultant output vector**
1	1	1	0	0	1	$\frac{4}{5}V_{dc}$
2	1	1	0	0	0	$\frac{4}{5}V_{dc}\exp(j0^0)$
3	1	1	1	0	0	$\frac{4}{5}V_{dc}\exp(j36^0)$
4	1	1	0	0	0	$\frac{4}{5}V_{dc}\exp(j72^0)$
5	0	1	1	0	0	$\frac{4}{5}V_{dc}\exp(j108^0)$
6	0	1	1	1	0	$\frac{4}{5}V_{dc}\exp(j144^0)$
7	0	0	1	1	0	$\frac{4}{5}V_{dc}\exp(j180^0)$
8	0	0	1	1	1	$\frac{4}{5}V_{dc}\exp(j216^0)$
9	0	0	0	1	1	$\frac{4}{5}V_{dc}\exp(j252^0)$
10	1	0	0	1	1	$\frac{4}{5}V_{dc}\exp(j288^0)$
11	1	0	0	0	1	$\frac{4}{5}V_{dc}\exp(j324^0)$

5. PREDICTIVE TORQUE CONTROL BASED FPSG

In this research paper the performance of Direct Torque Control (DTC) for FPSG with Predictive Torque Control (PTC) is compared in terms of stator current. DTC is used to decouple to control of stator flux and electromagnetic torque of FPSG during transient wind speed conditions. To implement DTC, separate closed control loops are required for stator flux and electromagnetic torque of FPSG. The closed control loops require PI- controllers to implement it. The elimination of usage of PI- controllers for controlling the stator flux and electromagnetic torque for FPSG a new control technique is proposed known as Predictive Torque Control (PTC) technique which results in reducing the ripple of the stator flux and electromagnetic torque. output of the generator.

The block diagram of PTC controlled FPSG shown in *figure 1* is presented. The main goal of Predictive Torque Control is to effectively regulate the torque generated by the FPSG, ensuring that it closely tracks a desired reference value in real-time. By use predictive modelling techniques to anticipate the future behavior of the system, while considering many limitations and objectives within a cost function [23]. the control algorithm computes the most efficient voltage vector references for each phase to get the targeted torque output.

6. PRINCIPLE OF OPERATION FOR PREDICTIVE TORQUE CONTROL WITH FPSG

The control system requires shown in *figure 1* requires reference torque during various wind speed variations and rated stator flux, which are typically determined by the wind turbine's power output requirements and operating conditions using machine side extrapolation equations. The mechanical power generated by the wind turbine as per the characteristics of wind turbine shown in *figure 3* are used to generated reference torque for the block diagram shown in *figure 1*. It requires two control loops such as stator flux control loop and torque control loop. In torque control loop it regulates the torque error by comparing the measured torque with the reference values. A torque controller, usually cost function for PTC to adjust the voltage applied for stator windings, processes the error signal. The Stator Flux Control loop regulates the stator flux error by comparing the measured stator flux with the reference values. The error signal is processed by a stator flux using cost function to adjust the voltage applied for stator windings.

The predictive torque controller is the core of the system. It uses mathematical models of $\lambda_{s,}^{p}(k+1), T_{e,}^{p}(k+1)$ used in *equation (18)* the of FPSG using machine side. The cost function is to predict the future behavior of the machine based on the current state and control actions. By simulating the system's response to various outer decagon voltage vectors, that minimizes the torque error and satisfies any operational constraints. Once the cost function minimizes the optimum voltage vector of outer decagon of five phase space vector diagram shown in *figure 4* is used to generate the appropriate switching signals for the inverter that drives the FPSG.

In discrete model stator flux connections are specified in terms of stator currents and rotor flux links. Stator currents and rotor flux linkages provided by the following equations which are

FOREX Publication
Open Access | Rapid and quality publishing
International Journal of Electrical and Electronics Research (IJEER)
Research Article | Volume 12, Issue 4 | Pages 1240-1250 | e-ISSN: 2347-470X

calculated by moving the variables in the one-sample Equation forward, [24] are used to determine future values for stator flux linkages using *equation (8)* and *equation (9).*

$$\lambda_{\alpha s}^{p}(k+1) = \sigma L_s i_{\alpha s}^{p}(k+1) + K_r \lambda_{\alpha r}^{p}(k+1) \quad (14)$$

$$\lambda_{\alpha r}^{p}(k+1) = \sigma L_s i_{\beta s}^{p}(k+1) + K_r \lambda_{\beta r}^{p}(k+1) \quad (15)$$

From the given model, the stator flux linkage peak value is calculated as in discrete time domain

$$\lambda_{\alpha s}^{p}(k+1) = \sqrt{\left[\lambda_{\alpha s}^{p}(k+1)\right]^2 + \left[\lambda_{\beta s}^{p}(k+1)\right]^2} \quad (16)$$

$$T_e^{p}(k+1) = 2.5\, P\, \lambda_{\alpha s}^{p}(k+1) i_{\beta s}^{p}(k+1) \quad (17)$$

Equations 16 and *equation 17* and reference values of stator flux and electromagnetic torque in are included in the cost function reference discrete time domain using equation 18 and is applied for 10 vectors of five phase space vector diagram shown in *figure 4* as follows, several parameters can be controlled simultaneously. The cost function uses *equation (18)* verifies each output voltage vector shown in *figure 4.* to minimize the errors between the reference value and actual values of stator flux and electromagnetic torque [24].

$$g_r(k) = \lambda_T\left[T_e^{*}(k+1) - T_e^{p}(k+1)\right]^2 + \lambda_\psi\left[\lambda_s^{*}(k+1) - \lambda_s^{p}(k+1)\right]^2 \quad (18)$$

$$\lambda_T = \frac{T_e}{T_e}\lambda_\psi = \frac{T_e}{\lambda_s}$$

Where λ_T is weighting factor for torque control and $\lambda\psi$ are is weighting factor for flux control.

The weighing factors are tuned for controlled stator flux and electromagnetic torque separately to minimize the error between actual and reference values.

7. TESTING OF FPSG WITH PTC TECHNIQUE USING MATLAB/SIMULINK

The proposed predictive torque control mathematical model of PTC for FPSG is tested at step change in wind speeds at 7.2 m/sec and 12 m/sec in MATLAB/ SIMULINK Environment for FPSG.

The simulation results for stator flux, five-phase stator fluxes, d and q–axis of stator currents, five-phase stator currents, electromagnetic torque and FFT Analysis with DTC and PTC techniques are presented.

To compare the harmonic analysis for stator currents of FPSG with DTC and PTC technique separate simulation was carried out for DTC technique in MATLAB/SIMULINK environment and the corresponding simulation results for DTC technique are also presented.

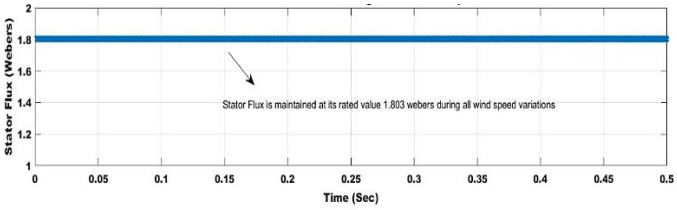

Figure 5. Stator Flux of FPSG using DTC technique

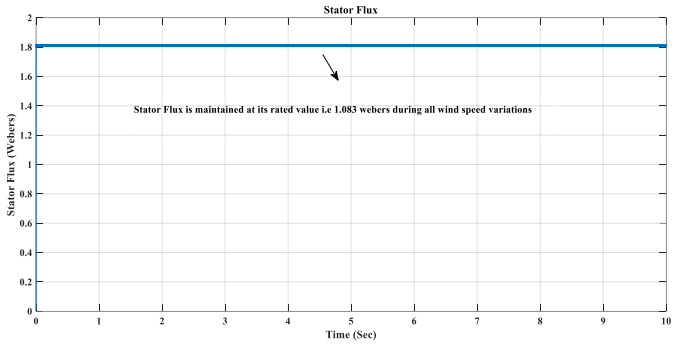

Figure 6. Stator Flux of FPSG with PTC technique

As per the objective of DTC and PTC technique it is observed that the stator flux is maintained at its rated value with DTC and PTC technique shown in *figures 5 and 6*. The ripple content of stator flux is reduced with PTC technique

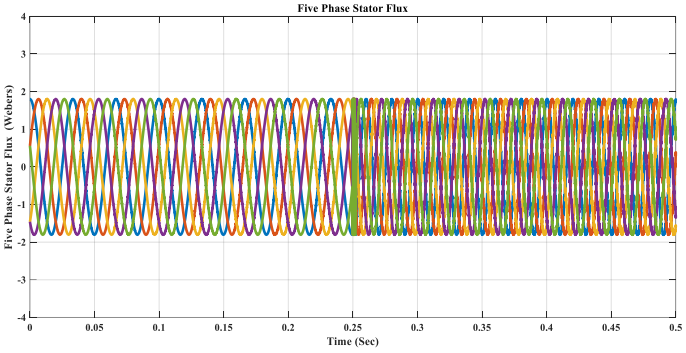

Figure 7. Five Phase Stator Fluxes of FPSG with DTC technique

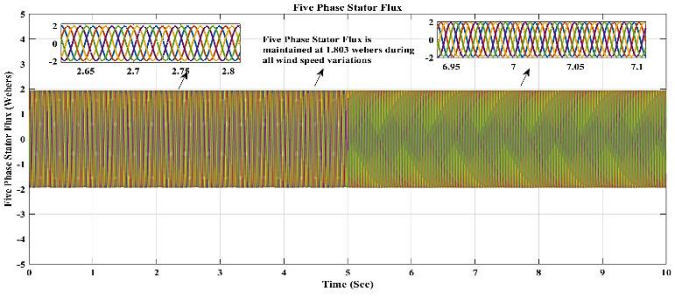

Figure 8. Five Phase Stator Fluxes of FPSG with PTC technique

Figures 7 and 8 it is observed that the five phase stator flux is maintained at its peak value of 1.803 Weber is due to constant flux shown in *figures 6 and 7* with DTC and PTC technique.

FOREX Publication
Open Access | Rapid and quality publishing
International Journal of Electrical and Electronics Research (IJEER)
Research Article | Volume 12, Issue 4 | Pages 1240-1250 | e-ISSN: 2347-470X

The ripple content of five phase stator flux is reduced with PTC technique.

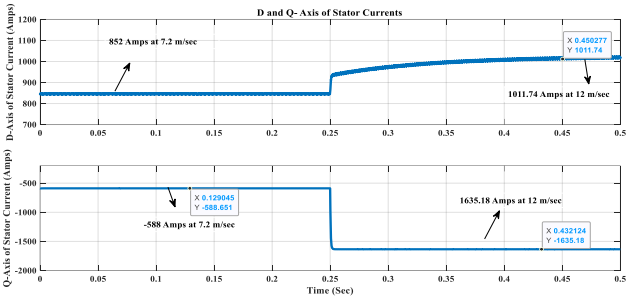

Figure 9. D and Q-axis of Stator Currents of FPSG with DTC technique

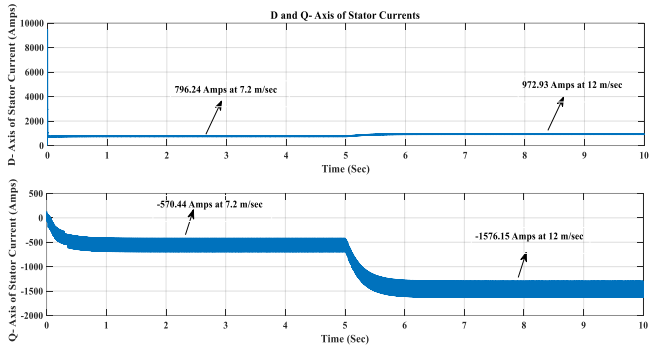

Figure 10. D axis and Q- axis of Stator Currents of FPSG with PTC technique

To maintain stator flux at its rated value shown in *figures 5 and 6* that the d-axis of stator current with value 883 Amps for 7.2 m/sec with DTC technique and 796.24A for 7.2 m/sec, with DTC technique and q- axis of stator currents are -1635.18 Amps with DTC and -1576.15 Amps with PTC techniques shown in *figures 9 and 10.*

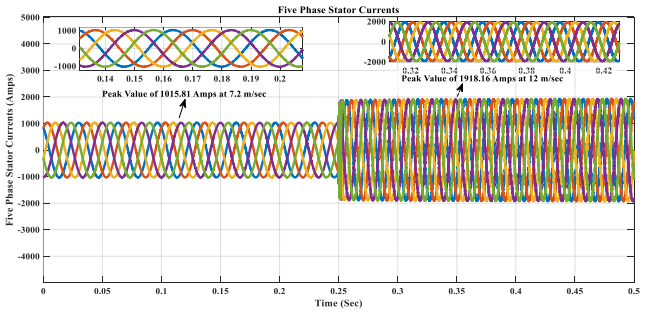

Figure 11. Five Phase Stator Currents of FPSG with DTC technique

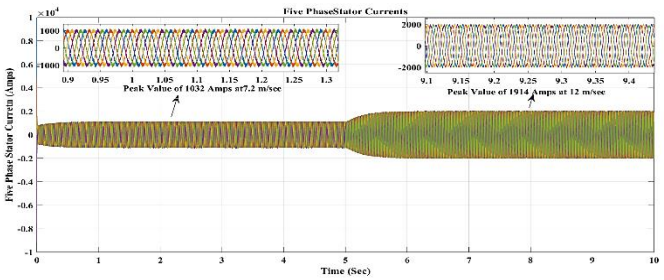

Figure 12. Five Phase Stator Currents of FPSG with PTC technique

Due to change in d and q- axis currents of the injected currents of FPSG during step change in wind speeds the five phase stator currents are varied with peak values of 1051.81 Amps for DTC and 1032 Amps with PTC technique at 7.2 m/sec at a frequency of 30HZ (0.6p.u of 50HZ), with peak values of 1918.16 Amps with DTC and 1914 Amps with PTC technique at 12 m/sec at 50 Hz (1 p.u) shown in *figures 11 and 12*.

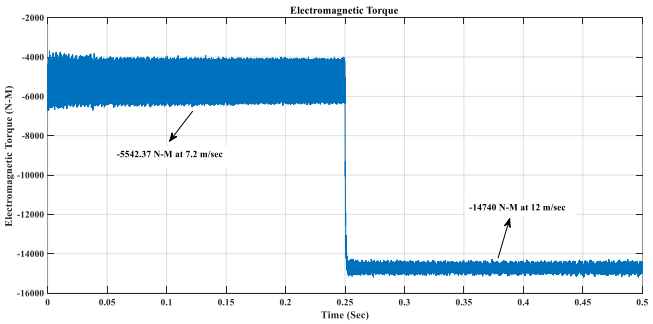

Figure 13. Electromagnetic Torque of FPSG with DTC technique

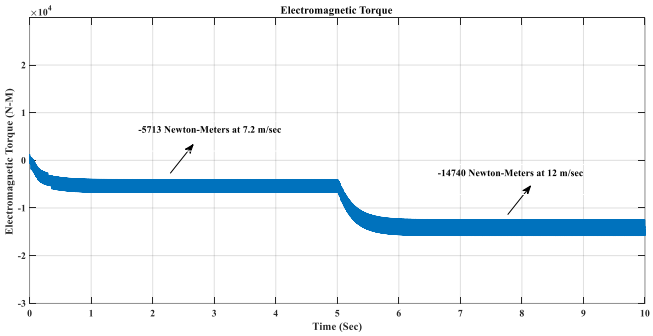

Figure 14. Electromagnetic Torque of FPSG with PTC technique

Due to change in q- axis of stator current shown in *figures 9 and 10* it is observed that electromagnetic torque of FPSG during every step change in wind speeds are -5306 N-M for 7.2 m/sec, - -14740 N-M for 12 m/sec. The ripple content of electromagnetic torque is reduced with PTC technique.

To analyse harmonics of stator current and grid current FFT analysis separate simulation is carried out for 7.2 m/sec and 12 m/sec wind speeds and the harmonic reduction is measured in terms of Total Harmonic Distortion (THD) for stator currents of FPSG with two level rectifier using DTC and PTC technique. The corresponding FFT analysis for FPSG with two level rectifier using DTC and PTC techniques are shown in *figures 15 to 18*. The harmonic analysis (THD) was done for state current (A-Phase) at 12 m/sec with DTC and PTC techniques.

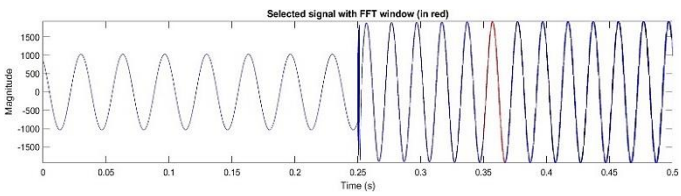

Figure 15. FFT for A- Phase Stator Current with DTC technique

International Journal of
Electrical and Electronics Research (IJEER)
Open Access | Rapid and quality publishing
Research Article | Volume 12, Issue 4 | Pages 1240-1250 | e-ISSN: 2347-470X

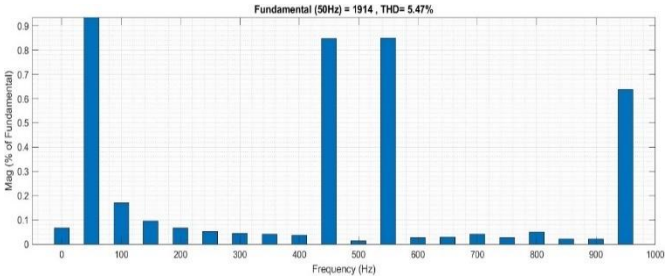

Figure 16. THD for A- Phase Stator Current with DTC technique

From the *figures 15 and 16* it is observed that the fundamental component of stator current is 1914 A with a THD of 5.47 with DTC technique.

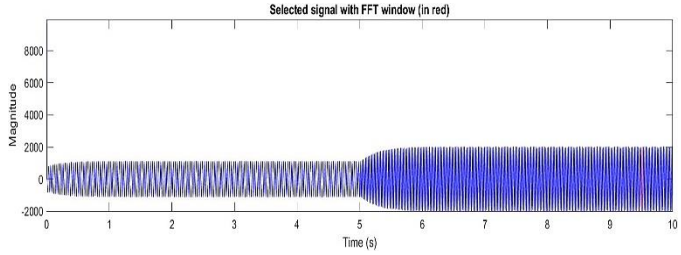

Figure 17. FFT for FPSG using PTC Technique

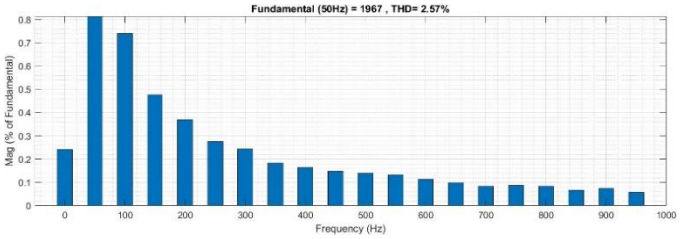

Figure 18.THD for FPSG using PTC Technique

From the *figures 17 and 18* it is observed that the fundamental component of stator current is 1967 A with a THD of 2.57.

Table 2. THD comparison of stator currents for PTC and DTC techniques

Component	Fundamental component (Amperes)	Total Harmonic Distortion (THD) %
FPSG with DTC with two level rectifiers (A-phase)	1914	5.47
FPSG with PTC two level rectifier (A-phase)	1967	2.57

From the FFT analysis, it is observed that THD component for stator current (A-Phase) is reduced to 2.57% from 5.47 in FPSG two level rectifier with PTC technique which is better than FPSG with two level rectifier using DTC.

8. CONCLUSION

The research paper titled "Minimization of Harmonic Reduction in Stator Current for Grid-Connected Five-Phase Squirrel Cage Induction Generator with Predictive Torque Control Technique" is a valuable addition to the field of power electronics and electric machine control. The suggested Predictive Torque Control (PTC) technique efficiently reduces harmonic distortion in the stator current of a five-phase squirrel cage induction generator (SCIG) when it is connected to the grid.

The results indicate that the PTC technique has a dual effect of improving power quality by reducing Total Harmonic Distortion (THD) and enhancing the dynamic performance of the generator. This approach demonstrates resilience under different operating conditions, providing enhanced regulation of the generator's torque and reducing stator current harmonics. The decreased harmonics result in lower strain on the electrical components, hence extending the lifespan of the generator and related equipment. This enhances the efficiency and dependability of the system for grid-connected applications.

In summary, the research offers a practical way to enhance the performance and efficiency of multi-phase induction generators. This has significant implications for renewable energy systems and other industrial applications that require the elimination of harmonics. Subsequent research could investigate the capabilities of this method to handle larger phase systems and its incorporation with further sophisticated control strategies to further improve the system's efficiency.

Appendix A
FPSG PARAMETERS

Power Rating	2.3 MW
Operating Voltage	690Volts
Frequency	50 Hz
Rated RPM	1512
No Of Poles	4
Rated Torque (N-M)	14740
Stator Resistance R_S	$1.102*10^{-3}$ ohms
Stator Inductance L_{ls}	$0.06492*10^{-3}$ Henry
Stator Flux λ_s	1.803 webers
Rotor Resistance R_r	$1.497*10^{-3}$ ohms
Rotor Flux λ_r	1.703 webers
Rotor Inductance L_{lr}	$0.06492*10^{-3}$ Henry
Mutual Inductance L_m	$2.13461*10^{-3}$ Henry
Moment of Inertia J	1200 Kg-m^2

REFERENCES

[1] Global Wind Energy Council, "Global Wind Report 2020," Global Wind Energy Council, Brussels, Belgium, 2020.

[2] B. Kirby, "Wind Power in Power Systems," IEEE Power and Energy Magazine, vol. 9, no. 6, pp. 36-42, Nov. 2011.

[3] J. G. Slootweg, H. Polinder, and W. L. Kling, "Representing Wind Turbine Electrical Generating Systems in Fundamental Frequency Simulations," IEEE Transactions on Energy Conversion, vol. 18, no. 4, pp. 516-524, Dec. 2003.

[4] D. V. G. Jayawardena and M. A. Masoum, "Wind Farms with Dynamic Reactive Power Control," IEEE Transactions on Power Systems, vol. 25, no. 2, pp. 667-676, May 2010.

FOREX Publication
Open Access | Rapid and quality publishing
International Journal of Electrical and Electronics Research (IJEER)
Research Article | Volume 12, Issue 4 | Pages 1240-1250 | e-ISSN: 2347-470X

[5] L. A. Barroso, H. Rudnick, G. C. Oliveira, and A. J. Conejo, "Wind Power and Market Power in Competitive Markets," IEEE Transactions on Power Systems, vol. 26, no. 2, pp. 807814, May 2011.

[6] A. Tapia, G. Tapia, J. X. Ostolaza, and J. R. Saenz, "Modeling and control of a wind turbine driven doubly fed induction generator," IEEE Transactions on Energy Conversion, vol. 18, no. 2, pp. 194-204, Jun. 2003.

[7] N. Bianchi, S. Bolognani, and E. Fornasiero, "Electrical machine topologies: State of the art and future trends," IEEE Transactions on Industrial Electronics, vol. 61, no. 6, pp. 58815895, Jun. 2014.

[8] S. S. Williamson, A. K. Rathore, and F. Musavi, "Industrial electronics for electric transportation: Current state-of-the-art and future challenges," IEEE Transactions on Industrial Electronics, vol. 62, no. 5, pp. 3021-3032, May 2015.

[9] E. Levi, "Multiphase electric machines for variable-speed applications," IEEE Transactions on Industrial Electronics, vol. 55, no. 5, pp. 1893-1909, May 2008.

[10] A. Iqbal and E. Levi, "Six-phase induction motor drive for harmonic cancellation," IEE Proceedings - Electric Power Applications, vol. 151, no. 6, pp. 744-752, Nov. 2004.
[11] M. Jones and E. Levi, "A literature survey of state-of-the-art in multiphase electric machines and drives," IEEE Transactions on Industry Applications, vol. 49, no. 2, pp. 924932, Mar.-Apr. 2013.

[12] I. Takahashi and T. Noguchi, "A new quick-response and high-efficiency control strategy of an induction motor," IEEE Transactions on Industry Applications, vol. IA-22, no. 5, pp. 820-827, Sep./Oct. 1986.

[13] G. S. Buja and M. P. Kazmierkowski, "Direct torque control of PWM inverter-fed AC motors—A survey," IEEE Transactions on Industrial Electronics, vol. 51, no. 4, pp. 744-757, Aug. 2004.

[14] M. Depenbrock, "Direct self-control (DSC) of inverter-fed induction machine," IEEE Transactions on Power Electronics, vol. 3, no. 4, pp. 420-429, Oct. 1988.

[15] R. Datta and V. T. Ranganathan, "Variable-speed wind power generation using doubly fed wound rotor induction machine—a comparison with alternative schemes," IEEE Transactions on Energy Conversion, vol. 17, no. 3, pp. 414-421, Sep. 2002.

[16] M. P. Kazmierkowski, R. Krishnan, and F. Blaabjerg, "Control in power electronics: selected problems," IEEE Transactions on Industrial Electronics, vol. 52, no. 3, pp. 615-622, Jun. 2005.

[17] P. Cortes, M. P. Kazmierkowski, R. M. Kennel, D. E. Quevedo, and J. Rodriguez, "Predictive control in power electronics and drives," IEEE Transactions on Industrial Electronics, vol. 55, no. 12, pp. 4312-4324, Dec. 2008.

[18] S. Kouro, M. Malinowski, K. Gopakumar, J. Pou, L. G. Franquelo, B. Wu, J. Rodriguez, M. A. Pérez, and J. I. Leon, "Recent advances and industrial applications of multilevel converters," IEEE Transactions on Industrial Electronics, vol. 57, no. 8, pp. 2553-2580, Aug. 2010.

[19] J. Rodriguez, P. Cortes, and C. Silva, "Predictive Control of Power Converters and Electrical Drives," IEEE Transactions on Industrial Electronics, vol. 56, no. 6, pp. 2100-2110, Jun. 2009.

[20] S. Vazquez, J. Pou, L. G. Franquelo, J. L. Leon, R. Portillo, M. A. Aguirre, and M. P. Kazmierkowski, "Model predictive control: A review of its applications in power electronics," IEEE Industrial Electronics Magazine, vol. 8, no. 1, pp. 16-31, Mar. 2014.

[21] A. K. Rathore, "High-performance control of induction motor drives for renewable energy applications," IEEE Transactions on Industry Applications, vol. 49, no. 5, pp. 2189-2197, Sep.Oct. 2013.

[22] P. Acuna, L. Moran, M. Rivera, J. R. Espinoza, and J. Rodriguez, "Predictive torque control of induction machines fed by indirect matrix converters with reactive power minimization," IEEE Transactions on Power Electronics, vol. 27, no. 11, pp. 4544-4553, Nov. 2012.

[23] B. K. Bose, “Modern Power Electronics and AC Drives,” Prentice Hall, Upper Saddle River, 2002. - References - Scientific Research Publishing.

[24] Venkata Yaramasu; Bin Wu “MPC of Wind Energy Conversion Systems”, ISBN: 9781118988589, July 2017.

[25] Iqbal, A., & Levi, E. (2006). Space Vector PWM Techniques for Sinusoidal Output Voltage Generation with a Five-Phase Voltage Source Inverter. Electric Power Components and Systems, 34(2), 119–140. https://doi.org/10.1080/15325000500244427

[26] Iqbal, Atif & Moin, Sk & Arif Khan, Mohd. (2010). Modeling, Simulation and Implementation of a Five-Phase Induction Motor Drive System. 2010 Joint International Conference on Power Electronics, Drives and Energy Systems, PEDES 2010 and 2010 Power India. 10.1109/PEDES.2010.5712373.

[27] E. Akbari and M. S. Shadlu, "A Novel Modified Fuzzy-Predictive Control of Permanent Magnet Synchronous Generator Based Wind Energy Conversion System," in Chinese Journal of Electrical Engineering, vol. 9, no. 4, pp. 107-121, December 2023, doi: 10.23919/CJEE.2023.000042.
[28] Y. Zhang, G. Li and M. Al-Ani, "Robust Learning-Based Model Predictive Control for Wave Energy Converters," in IEEE Transactions on Sustainable Energy, vol. 15, no. 3, pp. 1957-1967, July 2024, doi: 10.1109/TSTE.2024.3390394.

[29] N. Kayedpour, A. E. Samani, J. D. M. De Kooning, L. Vandevelde and G. Crevecoeur, "Model Predictive Control with a Cascaded Hammerstein Neural Network of a Wind Turbine Providing Frequency Containment Reserve," in IEEE Transactions on Energy Conversion, vol. 37, no. 1, pp. 198-209, March 2022, doi: 10.1109/TEC.2021.3093010.

[30] Y. Arias-Esquivel, R. Cárdenas, M. Diaz and L. Tarisciotti, "Continuous Control Set Model Predictive Control of a Hybrid Modular Multilevel Converter for Wind Energy Applications," in IEEE Transactions on Industrial Electronics, vol. 71, no. 11, pp. 14287-14297, Nov. 2024, doi: 10.1109/TIE.2024.3370982.

[31] L. Bigarelli, M. di Benedetto, A. Lidozzi, L. Solero, S. A. Odhano and P. Zanchetta, "PWM-Based Optimal Model Predictive Control for Variable Speed Generating Units," in IEEE Transactions on Industry Applications, vol. 56, no. 1, pp. 541-550, Jan.-Feb. 2020, doi: 10.1109/TIA.2019.2955662.

[32] P. Catalán, Y. Wang, J. Arza and Z. Chen, "Advanced Fault Ride-Through Operation Strategy Based on Model Predictive Control for High Power Wind Turbine," in IEEE Transactions on Sustainable Energy, vol. 15, no. 1, pp. 513-526, Jan. 2024, doi: 10.1109/TSTE.2023.3302770.

[33] K. R. Sekhar, R. Barot, P. Patel and N. V. Kumar, "A novel topology for improved DC bus utilization in PMSG based wind energy generation system," 2015 IEEE International Conference on Renewable Energy Research and Applications (ICRERA), Palermo, 2015, pp. 525-530.